

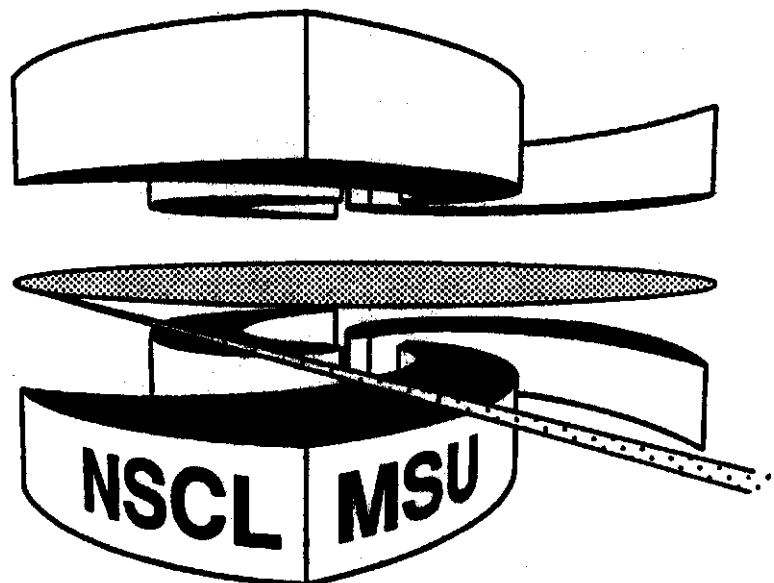


Michigan State University

National Superconducting Cyclotron Laboratory

**SQUEEZE-OUT OF NUCLEAR MATTER IN
Au + Au COLLISIONS**

**M.B. TSANG, P. DANIELEWICZ, W.C. HSI, H. HUANG,
W.G. LYNCH, D.R. BOWMAN, C.K. GELBKE, M.A. LISA,
G.F. PEASLEE, R.J. CHARITY, L.G. SOBOTKA,
M.L. BEGEMANN-BLAICH, F. COSMO, A. FERRERO,
J. HUBELE, G. IMME, I. IORI, J. KEMPTER, P. KREUTZ,
G.J. KUNDE, W.D. KUNZE, V. LINDENSTRUTH, U. LYNEN,
M. MANG, A. MORONI, W.F.J. MÜLLER, M. NEUMANN,
B. OCKER, C.A. OGLVIE, J. POCHODZALLA, G. RACITI,
F. ROSENBERGER, T. RUBEHN, H. SANN, R. SCARDAONI,
A. SCHÜTTAUF, C. SCHWARZ, W. SEIDEL, V. SERFLING,
W. TRAUTMANN, A. TUCHOLSKI, A. WÖRNER,
B. ZWIEGLINSKI; THE ALADIN COLLABORATION**



Squeeze-out of Nuclear Matter in Au + Au Collisions

M.B. Tsang, P. Danielewicz, W.C. Hsi, M. Huang, W.G. Lynch, D.R. Bowman',
C.K. Gelbke, M.A. Lisa**, and G.F. Peaslee'''

*Department of Physics and Astronomy and National Superconducting
Cyclotron Laboratory Michigan State University, East Lansing, MI 48824, USA,*

R. J. Charity and L.G. Sobotka

Department of Chemistry, Washington University; St. Louis, MO 63130, USA,

and

M.L. Begemann-Blaich^a, F. Cosmo^b, A. Ferrero^c, J. Hubele^a, G. Immed^d, I.
Iori^e, J. Kempter^a, P. Kreuz^a, G.J. Kunde^{a#}, W.D. Kunze^a, V. Lindenstruth^a,
U. Lynen^a, M. Mang^a, A. Moroni^c, W.F.J. Müller^a, M. Neumann^a, B. Ocker^a,
C.A. Ogilvie^{a##}, J. Pochodzalla^a, G. Raciti^d, F. Rosenberger^a, T. Rubehn^a, H.
Sann^a, R. Scardaoni^c, A. Schüttauf^a, C. Schwarz^a, W. Seidel^e, V. Serfling^a,
W. Trautmann^a, A. Tucholski^a, A. Wörner^a, B. Zwieglinski^f; the ALADIN
Collaboration

^a *Gesellschaft für Schwerionenforschung, D-6100 Darmstadt, Germany*

^b *Centre de Recherches Nucléaires, Strasbourg, France*

^c *INFN and Dipartimento di Fisica, Università degli Studi di Milano, I-20133,
Milano, Italy*

^d *INFN and Dipartimento di Fisica dell'Università, I-95129 Catania, Italy,*

^e *FZ Rossendorf, Dresden, Germany,*

^f *Soltan Institute for Nuclear Studies, Hoza, Warsaw, Poland*

Abstract

Emission of charged particles from a **compressed reaction zone** is studied for **$^{197}\text{Au} + ^{197}\text{Au}$ collisions** at $E/A = 100, 250,$ and 400 MeV . Using a **modified** coalescence invariant weighting, **squeeze-out** ratios; are **determined** and compared to predictions of cascade **and BUU transport-model** calculations.

PACS numbers: **25.70.Np, 25.70.Gh**

Hot and compressed nuclear matter may be momentarily created in the central participant region formed by the overlap of projectile and target nuclei during the early stages of energetic central nucleus-nucleus collisions [1-3]. Particles emitted near mid-rapidity originate preferentially from this hot and compressed reaction zone. The detailed emission pattern is influenced by rescattering and attenuation within the surrounding colder spectator matter. Particles emitted perpendicular to the reaction plane largely avoid this colder spectator matter and may therefore better reflect the conditions within the hot compressed zone.

The enhanced emission of mid-rapidity particles out of the reaction plane ("squeeze-out") has been investigated by determining aspect ratios of the flow tensor for light charged particles on an event by event basis and by studying the azimuthal distributions of these particles about the principal axis of the flow tensor [4]. Similar questions were addressed at incident energies of $E/A=400$ MeV by measuring the azimuthal distributions of the hydrogen isotopes and neutrons about the beam axis [5-8]. While these techniques provide comparable information for peripheral collisions where the flow axis (major axis of the flow tensor) is aligned closely with the beam axis, they differ for central and mid-central collisions where the flow θ_f angle may be large.

In general, comparisons to transport model calculations must account for the finite resolution with which the reaction plane is experimentally determined [1, 9,10]. However, the needed corrections are involved and have been rarely performed. By employing the mean tensor product technique discussed in detail in Ref. [11], one can determine the principal axes of the flow tensor without explicit determination of the reaction plane and, hence, avoid the sensitivity to the reaction plane dispersion. In this note, we present

the results of such an analysis for $^{197}\text{Au} + ^{197}\text{Au}$ collisions measured [12,13] at $E/A = 100, 250, \text{ and } 400 \text{ MeV}$.

The experiment was performed at the SIS facility at GSI. Gold targets of 3 and 5 mg/cm^2 areal density were used. Charged particles emitted to $14.5^\circ \leq \theta_{\text{lab}} \leq 160^\circ$ were detected in 225 plastic scintillator - CsI(Tl) phoswich detectors of the Miniball/Miniwall array [14]. By assuming a monotonically decreasing dependence of the charged particle multiplicity upon impact parameter, a reduced impact parameter scale, $\hat{b} = b/b_{\text{max}}$ (with $b_{\text{max}}=12.5 \text{ fm}$), was constructed from the charged particle multiplicity, N_C detected in the Miniball/Miniwall array [12]. The present squeeze-out analysis is restricted to particles with $1 \leq Z \leq 7$, $25^\circ \leq \theta_{\text{lab}} \leq 160^\circ$ and $5 \text{ MeV} \leq E/A \leq 75 \text{ MeV}$ for which the response of the CsI(Tl) detectors of the array is well understood; exceptions were deuterons and tritons which could only be analyzed up to $E/A = 50$ and 40 MeV , respectively. More details about the experiment can be found in Refs. [12,13].

Following Refs. [4,5,15], we define the flow tensor

$$S^{ij} = \sum_{\nu} W(\nu) p^i(\nu) p^j(\nu), \quad (1)$$

where $p^i(\nu)$ is the i^{th} component of the linear momentum vector of particle ν in the center-of-mass (CM) frame. In the present analysis, we use the weight

$$W(\nu) = \frac{Z(\nu)}{A(\nu)} \cdot \frac{1}{2m(\nu)} \quad (2)$$

where $Z(\nu)$ and $A(\nu)$ are the charge and mass numbers of particle ν and $m(\nu)$ is its mass. With this definition, the flow tensor is constructed from all detected protons (regardless of whether they are free or bound) in order to facilitate comparisons to transport models which do not incorporate cluster production.

The flow tensor S^{ij} characterizes the event by a triaxial ellipsoid in momentum space. The aspect ratios and orientation of this ellipsoid are calculated by diagonalizing the tensor and obtaining the eigenvalues ($\lambda_1, \lambda_2, \lambda_3$). By convention, axes 3 and 1 are the longer and shorter principal axes in the reaction plane, respectively, and axis 2 is the principal axis out of the plane; the flow angle, θ_f , is the angle between axis 3 and beam axis. In order to characterize participant particle emission to unshadowed regions out of plane one defines the squeeze-out ratio $R_\lambda = \lambda_2/\lambda_1$.

The orientation of the reaction plane of an event can be estimated from the direction of the transverse momentum vector

$$\mathbf{Q} = \sum_{\nu} \omega(\nu) \mathbf{p}^{\perp}(\nu) \quad (3)$$

where $\omega(\nu)$ is positive (negative) at positive (negative) rapidities in the CM frame, and $\mathbf{p}^{\perp}(\nu)$ is the particle's momentum component perpendicular to the beam. The choice $\omega(\nu) = W(\nu) p^z(\nu)$ yields the reaction plane associated with the principal axis of S^{ij} ; another common choice is $\omega(\nu) = y(\nu)/|y(\nu)|$ where $y(\nu)$ is the CM rapidity of the ν^{th} particle of the event [9]. When the directed transverse flow is weak (as is the case for rotating systems), the reaction plane can be estimated, alternatively, by diagonalizing the transverse momentum tensor [10,16].

In individual events, S^{ij} fluctuates significantly because of the finite number of particles. To reduce the sensitivity of the extracted values for R_λ to fluctuations, one may average the tensor over events, with the momentum of each particle rotated so that the reaction plane determined from the momenta of the other particles in the event coincide. This method does not eliminate uncertainties of the reaction plane determination, which must be assessed separately [9,17].

The "tensor product" technique of ref. [11] circumvents this problem. The technique is based upon the assumption that the dominant correlation between the particles' transverse momenta results from an anisotropy in the distribution of single-particle momentum components in the reaction plane. Under this assumption, the dot product of transverse momenta [11] may be approximated by:

$$\langle \mathbf{p}^\perp(\kappa_1) \cdot \mathbf{p}^\perp(\kappa_2) \rangle \approx \langle p^x(\kappa_1) \rangle \langle p^x(\kappa_2) \rangle \quad (4)$$

Here, κ is a variable which includes information about the rapidity and particle type (not to be confused with the particle index ν in Eqs. 1-3); $\langle p^x(\kappa_1) \rangle$ denotes the component of the mean transverse momentum in the reaction plane at rapidity $y_1(\eta)$ for a particle of species η . Introducing the rapidity weighting factor $\omega = y(\eta)/|y(\eta)|$ and extending this average over rapidity and particle species, we get

$$\langle \omega p^x \rangle^2 = \langle \omega(\kappa_1) p^\perp(\kappa_1) \cdot \omega(\kappa_2) p^\perp(\kappa_2) \rangle \quad (5)$$

for the square of the average transverse momentum, $\langle \omega p^x \rangle$. The average includes all pairs of particles regardless of particle type or rapidity. Similarly, $\langle S^{ij} \rangle$ can be derived from averages over tensor products of the momenta [11]:

$$\langle S^{zz} \rangle = \left\langle \sum_{\nu} W(\nu) p^z(\nu)^2 \right\rangle \quad (6)$$

$$\langle S^{xx} \rangle + \langle S^{yy} \rangle = \left\langle \sum_{\nu} W(\nu) p^\perp(\nu)^2 \right\rangle \quad (7)$$

$$\langle S^{xz} \rangle \langle \omega p^x \rangle = \left\langle \sum_{\nu\mu} W(\nu) \omega(\mu) p^z(\nu) p^\perp(\nu) \cdot p^\perp(\mu) \right\rangle / \left\langle \sum_{\mu} 1 \right\rangle \quad (8)$$

$$\{ \langle S^{yy} \rangle - \langle S^{xx} \rangle \} \langle \omega p^x \rangle^2 =$$

$$\left\langle \sum_{\nu\mu\gamma} W(\nu) \omega(\mu) \omega(\gamma) \left\{ p^\perp(\nu)^2 p^\perp(\mu) \cdot p^\perp(\gamma) - 2(p^\perp(\nu) \cdot p^\perp(\mu)) (p^\perp(\nu) \cdot p^\perp(\gamma)) \right\} \right\rangle / \left\langle \sum_{\mu\gamma} 1 \right\rangle$$

where the summations run over the detected particles and the averages run over all events. Squeeze-out ratios determined from Eqs. (5 - 9) do not suffer from uncertainties of the reaction plane reconstruction [11].

At the higher incident energies, the fixed experimental detector geometry restricts the usable rapidity region mainly to the backward hemisphere in the center of mass. Therefore, the squeeze-out ratios are determined from particles with $y < 0$. The open points in Fig. 1 show squeeze-out ratios, $R_\lambda = \lambda_2/\lambda_1$, obtained by averaging over events rotated to a common reaction plane. Magnitude and impact-parameter dependence of R_λ at $E/A = 250$ and 400 MeV are similar to values reported in Ref. [4] (except for the most peripheral collisions, for which the R_λ values of Ref. [4] diverged due to fluctuations). The solid points in Fig. 1 represent results obtained with the tensor product technique, Eqs. (5 - 9). Deviations from $R_\lambda = 1$ are larger when this latter method is used -- which may be expected because of its insensitivity to inaccuracies of the reaction plane reconstruction. Indeed, differences between the two methods are largest at $E/A = 100$ MeV where the reaction-plane reconstruction is poor because of the small magnitude of the sideward directed flow.

Squeeze-out ratios $R_\lambda > 1$ are consistent with a preferential emission of participant matter out of the reaction plane where it is not impeded by cold projectile and target-like matter. At $E/A = 100$ MeV, maximum squeeze-out occurs in central collisions. Values of $R_\lambda < 1$ are observed for larger impact parameters ($\hat{b} \geq 0.67$), indicating enhanced emission in the reaction plane. At $E/A = 400$ MeV, the maximum of R_λ shifts to mid-central collisions ($\hat{b} \approx 0.5$); further, $R_\lambda > 1$ for all values of \hat{b} .

Figure 2 illustrates the transition, at $E/A = 100$ MeV, from squeeze-out at small \hat{b} to a rotational flow pattern at large \hat{b} . The open points represent

azimuthal distributions about the beam axis [5,10,16] for particle emission at $\theta_{cm} = 70^\circ - 110^\circ$. Angles $\phi = 0^\circ$ and 180° correspond to emission in the reaction plane reconstructed, for central collisions, from the vector Q and, for peripheral collisions, by diagonalizing the transverse momentum tensor [10,16]. The direction $\phi = 0^\circ$ is defined from the projection of Q onto the reaction plane. Contributions of individual particles are weighted by Z , making the azimuthal distributions coalescence invariant. Peripheral collisions (left panel) exhibit a "V"-shaped azimuthal distribution reflecting strongly enhanced emission in the reaction plane. For central collisions (right panel), the azimuthal distribution has a broad maximum at $\phi = 90^\circ$ indicating a slightly enhanced emission out of the reaction plane. This enhanced out-of-plane emission can be shown more clearly by evaluating the azimuthal distribution [18] (solid points) about an average flow axis located at $\theta = 25^\circ$ in the reaction plane (determined from the other particles in an event to avoid autocorrelations).

For collisions at $E/A \geq 800$ MeV, the measured transverse flow could be reproduced by cascade calculations which assumed strict angular-momentum conservation, but neglected the nuclear mean field [19]. The dot-dot-dashed lines in the upper panels of Fig. 1 show the results of similar cascade calculations (filtered by our experimental acceptance). They fail to reproduce the measured energy dependence of R_λ and the in-plane enhancement ($R_\lambda < 1$) observed for peripheral collisions at $E/A = 100$ MeV.

Calculations with the Boltzmann-Uehling-Uhlenbeck (BUU) transport model (filtered by our experimental acceptance) are shown in the lower panels of Fig. 1. Besides nucleon-nucleon collisions modified by Pauli blocking, these calculations incorporate particle motion in a self-consistent mean field. The solid and dashed curves show predictions for a stiff ($K=375$

MeV) and a soft ($K=200$ MeV) equation of state (EOS) [1] using in-medium cross sections identical to the measured free nucleon-nucleon cross-sections, $\sigma_{NN} = \sigma_{free}$. The dot-dashed curves show the results of calculations for a stiff equation of state and reduced in-medium cross sections, $\sigma_{NN} = 0.8\sigma_{free}$. As expected, the BUU calculations provide better agreement with the data than the cascade calculations. The transition, at $E/A=100$ MeV, from enhanced out-of-plane to enhanced in-plane emission for increasing \hat{b} is reproduced, and quantitative agreement is obtained for the calculation with $\sigma_{NN} = 0.8\sigma_{free}$. (The 20% reduction of the cross sections is consistent with the reduction needed to fit the data on the balance energy [20].) At $E/A=250$, the agreement is best with the stiff EOS; all calculations are in good agreement with the data at $E/A = 400$ MeV. Overall, the sensitivity to the compressibility appears weak in this analysis because, in part, the current experiment cannot identify $Z = 1$ particles beyond 75 MeV/nucleon. If this restriction is removed from the calculations, the sensitivity to the compressibility at the higher incident energies and the lower impact parameters increases.

In summary, we have employed the tensor product technique of ref. [11] to extract squeeze-out ratios for Au+Au collisions at $E/A = 100, 250$ and 400 MeV. A transition from a squeeze-out to a rotational emission pattern as a function of impact parameter has been observed. The data are fairly well reproduced by BUU calculations, but not by cascade calculations. Comparison to BUU calculations shows that the squeeze-out ratios are sensitive to the in-medium nucleon-nucleon cross sections in collisions at $E/A=100$ MeV; this sensitivity is reduced at higher energies.

This work is supported by the National Science Foundation under Grant numbers PHY-90-15255, PHY-92-14992, and PHY-94-03666 and by the U.S. Department of Energy under Contract Nos. DE-FG02-87ER-40316 and FG06-

90ER40561. W.G. Lynch and L.G. Sobotka acknowledge the receipt of U.S. Presidential Young Investigator Awards. J.P. and M.B. acknowledge the financial support of the Deutsche Forschungsgemeinschaft under Contract No. Po256/2-1 and No. Be1634/1-1, respectively.

References:

- * Present Address: Chalk River Laboratories, Chalk River, Ontario K0J 1J0, Canada
 - ** Present Address: Lawrence Berkeley Laboratory, Berkeley, CA 94720, USA
 - *** Present Address: Physics Department, Hope College, Holland, MI 49423, USA
 - # Present Address: NSCL, Michigan State University, East Lansing, MI 48824, USA
 - ## Present Address: Department of Physics, MIT, Cambridge, MA 02139, USA
-
1. P. Danielewicz, *Phys. Rev. C* **51**, 716 (1995).
 2. H.H. Gutbrod, A.M. Poskanzer, and H.G. Ritter, *Rep. Prog. Phys.* **52**, 1267 (1989).
 3. H. Stöcker and W. Greiner, *Phys. Rep.* **137**, 277 (1986).
 4. H.H. Gutbrod, K.H. Kampert, B. Kolb, A.M. Poskanzer, H.G. Ritter, R. Schicker, and H.R. Schmidt, *Phys. Rev. C* **42**, 640 (1990).
 5. H.H. Gutbrod, K.H. Kampert, B.W. Kolb, A.M. Poskanzer, H.G. Ritter, and H.R. Schmidt, *Phys. Lett. B* **216**, 267 (1989).
 6. M. Elaasar, R. Madey, W.M. Zhang, J. Schambach, D. Keane, B.D. Anderson, A.R. Baldwin, J.W. Watson, G.D. Westfall, G. Krebs, H. Wieman, C. Gale, K. Haglin, *Phys. Rev. C* **49**, R10 (1994).
 7. Y. Leifels, Th. Blaich, Th.W. Elze, H. Emling, H. Freiesleben, K. Grimm, W. Henning, R. Holzmann, J.G. Keller, H. Klingler, J.V. Kratz, R. Kulesa, D. Lambrecht, S. Lange, E. Lubkiewicz, E.F. Moore, W. Prokopowicz, R. Schmidt, C. Schütter, H. Spies, K. Stelzer, J. Stroth, E. Wajda, W. Walus,

- M. Zinser, E. Zude, and the FOPI-Collaboration, *Phys. Rev. Lett.* **71**, 963 (1993).
8. R.A. Popescu, J.C. Angélique, G. Auger, G. Bizard, R. Brou, A. Buta, C. Cabot, E. Crema, D. Cussol, Y. El Masri, P. Eudes, M. Gonin, K. Hagel, Z.Y. He, A. Kerambrun, C. Lebrun, J.P. Patry, A. Péghaire, J. Péter, R. Régimbart, E. Rosato, F. Saint-Laurent, J.C. Steckmeyer, B. Tamain, E. Vient, and R. Wada, *Phys. Lett.* **B331**, 285 (1994).
 9. P. Danielewicz and G. Odyniec, *Phys. Lett.* **B157**, 146 (1985).
 10. M.B. Tsang, R.T. de Souza, Y.D. Kim, D.R. Bowman, N. Carlin, C.K. Gelbke, W.G. Gong, W.G. Lynch, L. Phair, and F. Zhu, *Phys. Rev.* **C44**, 2065 (1991).
 11. P. Danielewicz, H. Ströbele, G. Odyniec, D. Bangert, R. Bock, R. Brockmann, J.W. Harris, H.G. Pugh, W. Rauch, R.E. Renfordt, A. Sandoval, D. Schall, L.S. Schroeder, and R. Stock, *Phys. Rev.* **C38**, 120 (1988).
 12. W.C. Hsi, G.J. Kunde, J. Pochodzalla, W.G. Lynch, M.B. Tsang, M.L. Begemann-Blaich, D.R. Bowman, R.J. Charity, A. Cosmo, A. Ferrero, C.K. Gelbke, T. Glasmacher, T. Hofmann, G. Immé, I. Iori, J. Hubele, J. Kempter, P. Kreuzt, W.D. Kunze, V. Lindenstruth, M.A. Lisa, U. Lynen, M. Mang, A. Moroni, W.F.J. Müller, M. Neumann, B. Ocker, C.A. Ogilvie, G.F. Peaslee, G. Raciti, F. Rosenberger, H. Sann, R. Scardaoni, A. Schüttauf, C. Schwarz, W. Seidel, V. Serfling, L.G. Sobotka, L. Stuttge, S. Tomasevic, W. Trautmann, A. Tucholski, C. Williams, A. Wörner, and B. Zwieglinski, *Phys. Rev. Lett.* **73**, 3367 (1994).
 13. M.B. Tsang, W.C. Hsi, W.G. Lynch, D.R. Bowman, C.K. Gelbke, M.A. Lisa, G.F. Peaslee, G.J. Kunde, M.L. Begemann-Blaich, T. Hofmann, J. Hubele, J. Kempter, P. Kreuzt, W.D. Kunze, V. Lindenstruth, U. Lynen, M. Mang,

- W.F.J. Müller, M. Neumann, B. Ocker, C.A. Ogilvie, J. Pochodzalla, F. Rosenberger, H. Sann, A. Schüttauf, V. Serfling, J. Stroth, W. Trautmann, A. Tucholski, A. Wörner, E. Zude, B. Zwieglinski, S. Aiello, G. Immé, V. Pappalardo, G. Raciti, R.J. Charity, L.G. Sobotka, I. Iori, A. Moroni, R. Scardoni, A. Ferrero, W. Seidel, Th. Blaich, L. Stuttge, A. Cosmo, W.A. Friedman, and G. Peilert, *Phys. Rev. Lett.* **71**, 1502 (1993).
14. R.T. de Souza, N. Carlin, Y.D. Kim, J. Ottarson, L. Phair, D.R. Bowman, C.K. Gelbke, W.G. Gong, W.G. Lynch, R.A. Pelak, T. Peterson, G. Poggi, M.B. Tsang, and H.M. Xu, *Nucl. Instr. and Meth.* **A295**, 109 (1990).
 15. H.A. Gustafsson, H.H. Gutbrod, B. Kolb, H. Löhner, B. Ludewigt, A.M. Poskanzer, T. Renner, H. Riedesel, H.G. Ritter, A. Warwick, F. Weik, and H. Wieman, *Phys. Rev. Lett.* **52**, 1590 (1984).
 16. W.K. Wilson, W. Benenson, D.A. Cebra, J. Clayton, S. Howden, J. Karn, T. Li, C.A. Ogilvie, A. Vander Molen, G.D. Westfall, J.S. Winfield, B. Young, and A. Nadasen, *Phys. Rev.* **C41**, R1881 (1990).
 17. J.P. Sullivan and J. Péter, *Nucl. Phys.* **A540**, 275 (1992).
 18. To correct for azimuthally dependent detection efficiencies, this distribution was divided by the instrumental anisotropy obtained by a parallel analysis which assumes a random azimuthal orientation of the reaction plane.
 19. D.E. Kahana, D. Keane, Y. Pang, T. Schlagel, and S. Wang, *Phys. Rev. Lett.* **74**, 4404 (1995).
 20. G.D. Westfall, W. Bauer, D. Craig, M. Cronqvist, E. Gualtieri, S. Hannuschke, D. Klakow, T. Li, T. Reposeur, A.M. Vander Molen, W.K. Wilson, J.S. Winfield, J. Yee, S.J. Yennello, R. Lacey, A. Elmaani, J. Lauret, A. Nadasen, E. Norbeck, *Phys. Rev. Lett.* **71**, 1986 (1993).

Figure Captions :

Fig. 1: Measured squeeze-out ratios as a function of reduced impact parameter for Au+Au collisions at $E/A = 100, 250$ and 400 MeV. Solid points are obtained with the tensor product method (Eqs. 5- 9). Open points are obtained by rotating the events individually to a common reaction plane (method 2 described in the text). The curves in the top and bottom panels show results of cascade and BUU calculations, respectively. The BUU calculations were performed for in medium cross sections $\sigma_{NN} = \sigma_{free}$ using a stiff (solid curves) or soft (dashed curves) equation of state, and for $\sigma_{NN} = 0.8\sigma_{free}$ using a stiff equation of state.

Fig. 2: Azimuthal distributions of the emitted particles for Au+Au collisions at $E/A=100$ MeV for peripheral (left panel) and central (right panel) collisions.

$^{197}\text{Au} + ^{197}\text{Au}$

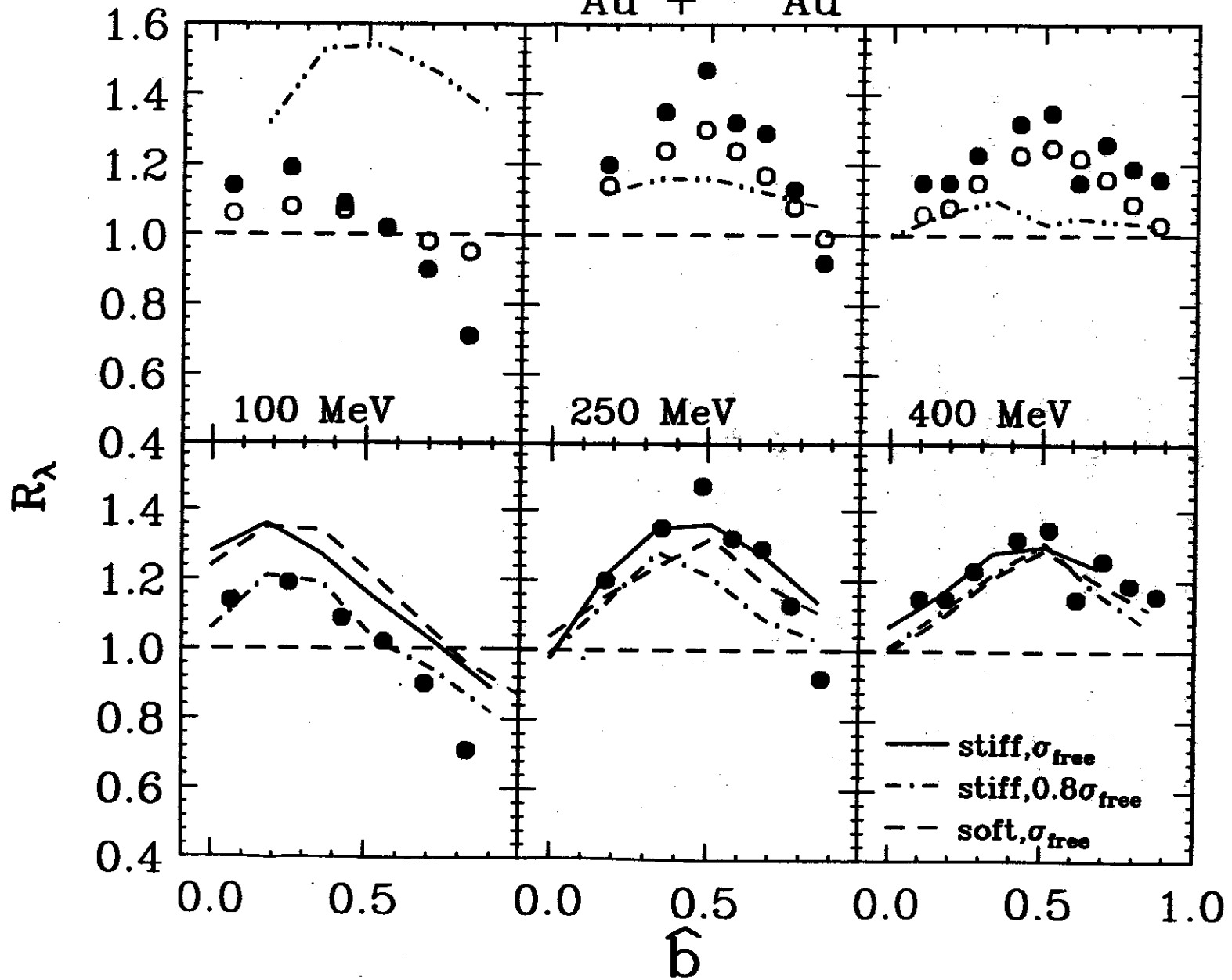


Fig. 1

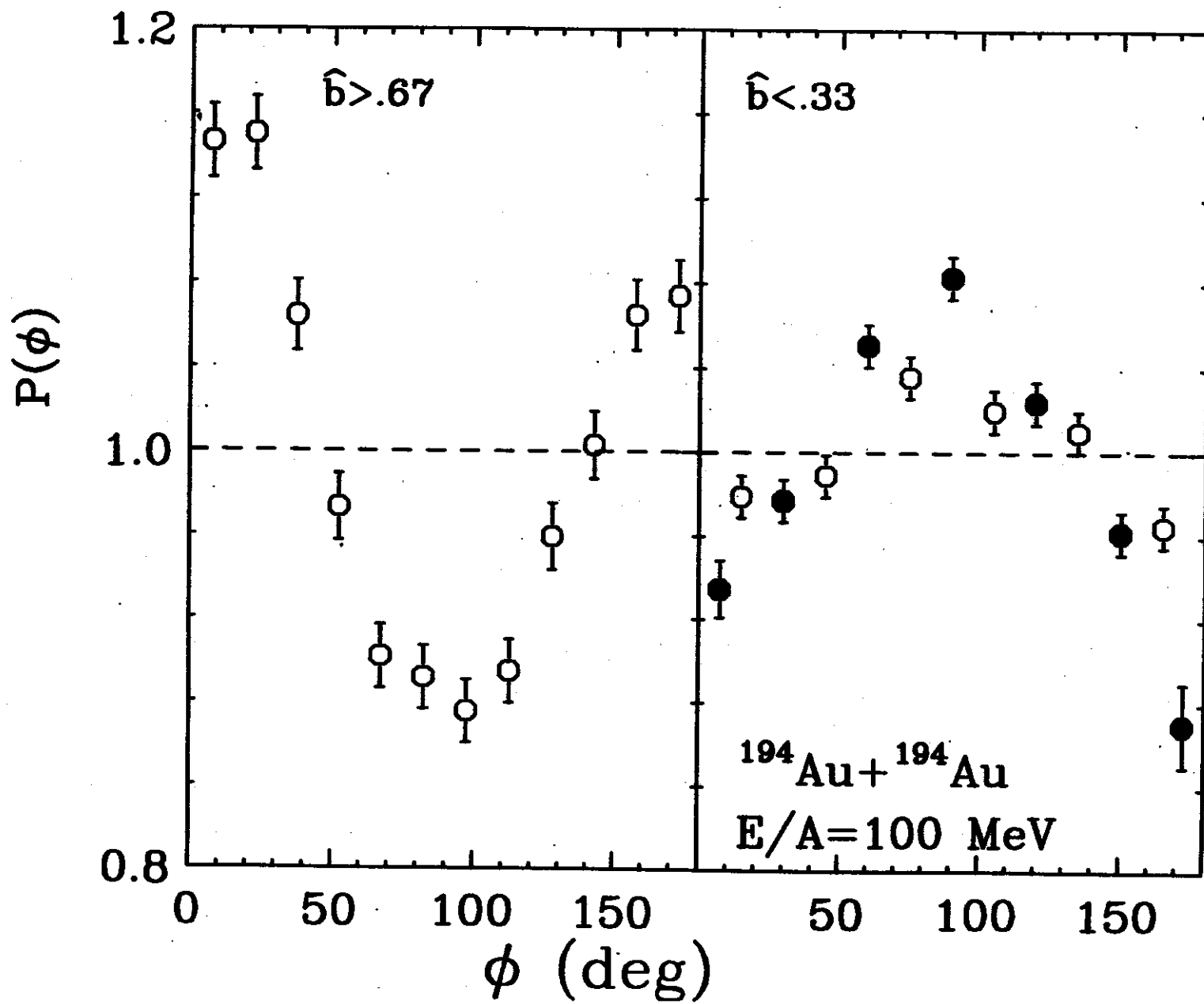


Fig. 2